

**Daniel A. Dombeck, Leonardo Sacconi, Mireille Blanchard-Desce and Watt W. Webb**

*J Neurophysiol* 94:3628-3636, 2005. First published Aug 10, 2005; doi:10.1152/jn.00416.2005

**You might find this additional information useful...**

---

This article cites 43 articles, 13 of which you can access free at:

<http://jn.physiology.org/cgi/content/full/94/5/3628#BIBL>

This article has been cited by 4 other HighWire hosted articles:

**Polarized microtubule arrays in apical dendrites and axons**

A. C. Kwan, D. A. Dombeck and W. W. Webb  
*PNAS*, August 12, 2008; 105 (32): 11370-11375.  
[\[Abstract\]](#) [\[Full Text\]](#) [\[PDF\]](#)

**Dendritic signals from rat hippocampal CA1 pyramidal neurons during coincident pre- and post-synaptic activity: a combined voltage- and calcium-imaging study**

M. Canepari, M. Djuricic and D. Zecevic  
*J. Physiol.*, April 15, 2007; 580 (2): 463-484.  
[\[Abstract\]](#) [\[Full Text\]](#) [\[PDF\]](#)

**Overcoming photodamage in second-harmonic generation microscopy: Real-time optical recording of neuronal action potentials**

L. Sacconi, D. A. Dombeck and W. W. Webb  
*PNAS*, February 28, 2006; 103 (9): 3124-3129.  
[\[Abstract\]](#) [\[Full Text\]](#) [\[PDF\]](#)

**Imaging membrane potential in dendritic spines**

M. Nuriya, J. Jiang, B. Nemet, K. B. Eisenthal and R. Yuste  
*PNAS*, January 17, 2006; 103 (3): 786-790.  
[\[Abstract\]](#) [\[Full Text\]](#) [\[PDF\]](#)

Updated information and services including high-resolution figures, can be found at:

<http://jn.physiology.org/cgi/content/full/94/5/3628>

Additional material and information about *Journal of Neurophysiology* can be found at:

<http://www.the-aps.org/publications/jn>

---

This information is current as of July 12, 2009 .

# Optical Recording of Fast Neuronal Membrane Potential Transients in Acute Mammalian Brain Slices by Second-Harmonic Generation Microscopy

Daniel A. Dombeck,<sup>1</sup> Leonardo Sacconi,<sup>1,2</sup> Mireille Blanchard-Desce,<sup>3</sup> and Watt W. Webb<sup>1</sup>

<sup>1</sup>School of Applied and Engineering Physics, Cornell University, Ithaca, New York; <sup>2</sup>European Laboratory for Non-Linear Spectroscopy, University of Florence, Sesto Fiorentino, Florence, Italy; and <sup>3</sup>Synthese et Electrochimie Organiques, Centre National de la Recherche Scientifique, Institut de Chimie, Université de Rennes 1, Rennes, France

Submitted 25 April 2005; accepted in final form 4 August 2005

**Dombeck, Daniel A., Leonardo Sacconi, Mireille Blanchard-Desce, and Watt W. Webb.** Optical recording of fast neuronal membrane potential transients in acute mammalian brain slices by second-harmonic generation microscopy. *J Neurophysiol* 94: 3628–3636, 2005. First published August 10, 2005; doi:10.1152/jn.00416.2005. Although nonlinear microscopy and fast ( $\sim 1$  ms) membrane potential ( $V_m$ ) recording have proven valuable for neuroscience applications, their potentially powerful combination has not yet been shown for studies of  $V_m$  activity deep in intact tissue. We show that laser illumination of neurons in acute rat brain slices intracellularly filled with FM4-64 dye generates an intense second-harmonic generation (SHG) signal from somatic and dendritic plasma membranes with high contrast  $>125 \mu\text{m}$  below the slice surface. The SHG signal provides a linear response to  $\Delta V_m$  of  $\sim 7.5\%/100$  mV. By averaging repeated line scans ( $\sim 50$ ), we show the ability to record action potentials (APs) optically with a signal-to-noise ratio (S/N) of  $\sim 7$ – $8$ . We also show recording of fast  $V_m$  steps from the dendritic arbor at depths inaccessible with previous methods. The high membrane contrast and linear response of SHG to  $\Delta V_m$  provides the advantage that signal changes are not degraded by background and can be directly quantified in terms of  $\Delta V_m$ . Experimental comparison of SHG and two-photon fluorescence  $V_m$  recording with the best known probes for each showed that the SHG technique is superior for  $V_m$  recording in brain slice applications, with FM4-64 as the best tested SHG  $V_m$  probe.

## INTRODUCTION

Measuring electrical phenomenon of excitable cells is vital to understanding both their intrinsic and network properties. These recordings are still predominantly accomplished through the use of microelectrodes, which are generally limited to recording from only a few positions in a sample (Stuart and Sakmann 1994). Optical methods of recording  $V_m$  allow for multiple site recordings from populations, single cells, and fine processes that are too small or fragile for electrode recordings (Grinvald and Hildesheim 2004; Zochowski et al. 2000).

Current optical techniques to record fast  $V_m$  events in neural systems rely on one-photon methods (Antic 2003; Cohen et al. 1968; Gonzalez and Tsien 1997; Knopfel et al. 2003; Siegel and Isacoff 1997; Stepnoski et al. 1991; Zochowski et al. 2000) (fluorescence, absorption, etc.). One-photon fluorescence methods can be used to generate high signal-to-noise ratio (S/N) measurements of action potentials (APs) from subcellular regions in a single trial (Antic 2003; Antic and Zecevic 1995; Milojkovic et al. 2004) and subthreshold events with averaging (Antic and Zecevic 1995; Djuricic et al. 2004). Such

recordings have been made from neurons in superficial layers of thick specimens (Antic 2003; Djuricic et al. 2004; Milojkovic et al. 2004); however, these techniques are generally limited by light scattering to depths less than  $\sim 50 \mu\text{m}$  below the surface. To record  $V_m$  activity optically deep in intact systems with high spatial resolution, nonlinear optical methods [second-harmonic generation (SHG) or two-photon fluorescence (TPF)] are needed (Denk and Svoboda 1997; Denk et al. 1990; Dombeck et al. 2003; Kuhn et al. 2004; Mertz 2004; Zipfel et al. 2003a). The challenges of observing fast ( $\sim 1$  ms)  $V_m$  events with nonlinear microscopy are significant, mainly because of the relatively small number of photons collected per time-point. The corresponding shot noise places strict limitations on the level of detectable signals and dye response to  $\Delta V_m$  that are needed. Compounding this problem for TPF is the reduction in the measured dye response to  $\Delta V_m$  by dye molecules that are present within the focal volume but are not embedded in the plasma membrane (background). Variations in this background can have the effect of making the observed  $\Delta F/F$  signal difficult to quantify in terms of  $\Delta V_m$  unless the background can be kept low (as in culture; Bullen and Saggau 1999) or unless prior knowledge of the cellular  $V_m$  properties exists (Djuricic et al. 2004).

SHG has the potential to solve these problems. Because of the molecular alignment requirement for signal generation of this coherent two-photon scattering process, the SHG signal only emanates from properly oriented dye molecules in the membrane (Bouevitch et al. 1993; Campagnola et al. 1999; Mertz and Moreaux 2001); thus its effective  $V_m$  response is not significantly attenuated by background. The high membrane contrast also allows for a more direct relation between optical signal change and  $\Delta V_m$ . As with TPF, the nonlinear nature of SHG provides optical sectioning and micron scale resolution at depths up to  $\sim 400 \mu\text{m}$  into scattering brain tissue (Dombeck et al. 2003).

Fast SHG recordings of  $\Delta V_m$  have been achieved in model membranes (Moreaux et al. 2003; Pons et al. 2003) and *Aplysia* neurons in culture (Dombeck et al. 2004), but have not yet been applied to intact mammalian neural systems where the full advantages could be realized. Previous SHG studies were also restricted to dyes that could only label cells extracellularly and could not be intracellularly applied with a pipette. Here we report on the latest step toward high-resolution SHG imaging

Address for reprint requests and other correspondence: W. W. Webb, Applied Physics, Cornell Univ., 223 Clark Hall, Ithaca, NY 14853 (E-mail: www2@cornell.edu).

The costs of publication of this article were defrayed in part by the payment of page charges. The article must therefore be hereby marked "advertisement" in accordance with 18 U.S.C. Section 1734 solely to indicate this fact.

of  $V_m$  in thick preparations by labeling a specifically targeted mammalian neuron below superficial layers in brain slices through intracellular application of FM4-64. We show the use of SHG microscopy for recording APs and fast voltage steps deep in slice where other techniques are not effective. For a direct comparison between SHG and TPF  $V_m$  recording in optically thick preparations, we optically record fast  $V_m$  signals with the two methods in brain slices using the best known  $V_m$  probes. We found the FM4-64 SHG S/N and effective  $V_m$  response to be greater than that for any other tested SHG or TPF probe. Even though TPF can outperform SHG in the culture dish, SHG is superior in brain slice systems because of its low background and high plasma membrane contrast compared with TPF.

## METHODS

### FM4-64 brain slice recordings

**IMAGING.** The basic design of our Radiance 2000 (Bio-Rad)-based imaging system has been described (Dombeck et al. 2003, 2004). Now, however, an upright microscope (BX50WI, Olympus) is used with a 0.8-NA condenser for infrared video microscopy and collection of the transmitted SHG signal, 530/30 and 580/150 optical filters (Chroma Technology) for SHG and TPF detection, respectively, and GaAsP PMTs (H7422, Hamamatsu) for signal detection. A physiology objective ( $\times 40$ , 0.8 NA, overfilled back aperture) was used for illumination and epi (backward) collection. Excitation was provided by a  $1,064 \pm 15$ -nm fiber laser (Fianium, FEMPTOPOWER 1060) with  $\sim 300$ -fs pulses at 70 MHz,  $\sim 10$ - to 20-mW average power, and near linear polarization at the sample. This excitation was used instead of shorter wavelengths ( $\sim 900$  nm) because 1) greater SHG responses to  $\Delta V_m$  were observed at 1,064 ( $\sim 7.5\%/100$  mV) than 900 nm ( $\sim 5\%/100$  mV); 2) absorption by intrinsic flavins will affect the 450-nm SHG signal more than the 532-nm signal; and 3) the quantum efficiency of available photodetectors is higher using GaAsP PMTs to collect 532-nm light ( $\sim 40\%$ ) than using BiAlkali PMTs to collect 450-nm light ( $\sim 25\%$ ) (Zipfel et al. 2003b).

**SLICE PREPARATION.** Animals were treated in accordance with Cornell University Regulations (IACUC protocol 00-46-03). Transverse brain slices ( $\sim 250$   $\mu$ m thick) were made with a vibratome (Integraslice 7550 PSDS, Campden Instruments) from Sprague-Dawley rats (P5–P25) in 4°C oxygenated sucrose slicing solution (Kirov et al. 2004) containing (in mM) 212 sucrose, 25 NaHCO<sub>3</sub>, 2.5 KCl, 1.25 NaH<sub>2</sub>PO<sub>4</sub>, 2 CaCl<sub>2</sub>, 1 MgCl<sub>2</sub>, and 25 glucose (pH 7.4; osmolarity,  $\sim 310$  mosmol/l). Slices were transferred to an  $\sim 35^\circ$ C oxygenated extracellular solution containing (in mM) 125 NaCl, 25 NaHCO<sub>3</sub>, 2.5 KCl, 1.25 NaH<sub>2</sub>PO<sub>4</sub>, 2 CaCl<sub>2</sub>, 1 MgCl<sub>2</sub>, and 25 glucose (pH 7.4; osmolarity,  $\sim 310$  mosmol/l with glucose). The slices were allowed to rest at 35°C for 30 min before being moved to room temperature until use.

**ELECTROPHYSIOLOGY, STAINING, AND LINE SCANNING.** Slices were transferred to a recording chamber continually perfused with warm ( $35 \pm 1^\circ$ C) oxygenated extracellular solution. Whole cell patch-clamp recordings were obtained under infrared video microscopy using an Axoclamp 2b amplifier (Axon Instruments) and 5–10 M $\Omega$  pipettes filled with intracellular solution containing (in mM) 130 K-Gluconate, 5 NaCl, 24 KCl, 10 HEPES, 4 Mg-ATP, and 0.4 Na-GTP (pH 7.3 with KOH; osmolarity,  $\sim 305$  mosmol/l). A final concentration of 200  $\mu$ M FM4-64 was added to this solution, sonicated for  $\sim 1$  min, and passed through a 0.2- $\mu$ m filter to remove any dye precipitate. Once a gigaohm seal was obtained, quick negative pressure pulses opened the seal for whole cell recording and dye filling. Neurons from the dentate gyrus (DG), CA1, and entorhinal cortex were used, but not identified,

except by physical location. Advasep 7 (1 mM; Cydex) was added to the extracellular solution. As expected, this absorbs dye discharged into the neural tissue when obtaining a patch and likely any dye that flip-flops to the outer plasma membrane leaflet during the course of the experiments (Kay et al. 1999). SHG population labeling with dye crystals has been shown (Mertz and Moreaux 2001), but here deeper labeling was accomplished by pressure ( $\sim 50$  mmHg) injecting (Stosiek et al. 2003)  $\sim 500$   $\mu$ M FM4-64 in extracellular solution into the tissue through a patch pipette for  $\sim 1$ –5 min.

TTL pulse triggering was used to synchronize the electrophysiology stimuli to each line scan (triggering jitter  $< 3$   $\mu$ s). Data were collected during the scanning fly-back to obtain line scanning rates of 1,200 lines/s for AP recordings, whereas unidirectional scanning (300 and 600 lines/s, no fly-back collection) was used for dendrite recordings; 200–256 lines were collected per individual line scan. Two to 5 s were allowed between the 35–60 individual line scans that were later averaged, with typical AP averaging taking  $\sim 2$  min and voltage step averaging on dendrites taking  $\sim 3$  min. APs were elicited in current clamp during individual line scans by current injection through the pipette. Stimulation of APs was possible with  $\sim 200$ -pA and  $\sim 8$ -ms pulses; however, shorter pulses of more intense current ( $\sim 1$  nA,  $\sim 1$ -ms duration) were used to reach threshold quickly. This stimulation protocol led to a greater AP temporal stability of less than  $\sim 0.2$ -ms drift over the minutes of signal averaging not possible with the longer protocol (more than  $\sim 2$ -ms drift). This was necessary to synchronize the timing of the short-duration APs with the time during which the SHG was collected per line; this synchronization protocol has been previously described (Dombeck et al. 2004). The electrode recorded APs shown in Fig. 3C are the mean of  $n = 55$ . This averaging can have the effect of reducing AP amplitudes by  $\sim 10$ –15% and increasing AP durations up to  $\sim 10$ –20% compared with single trace recordings because of the small temporal drift of the APs from trial to trial. Voltage steps were applied in voltage clamp during line scans.

A  $V_m$ -independent bleaching effect during each individual line scan ( $\sim 1$ –5%/100 ms) was observed; this distortion to the SHG time-course was normalized from the recordings by fitting with a mono-exponential decay. The time allowed between individual line scans (2–5 s) was sufficient for nonbleached dye to diffuse and replenish the scanned membrane region. Preliminary reports of research using SHG from intracellularly filled FM4-64 to detect  $\Delta V_m$  in brain slices have been published in abstract form (Dombeck et al. 2005a,b; Yuste et al. 2005).

### Comparison of various SHG and TPF probes

The most important parameter for comparing various dyes for optical  $V_m$  recording is the S/N; we attempted to maximize this value for each tested dye as follows. The S/N is proportional to the  $V_m$  sensitivity ( $\Delta S/S$ ) and the square root of the photon flux (see Eq. 1). Therefore the dye concentration and wavelength for each specific dye was selected either to produce the highest photon flux and  $\Delta S/S$ , respectively, or to reproduce previous studies by other researchers. We varied the illumination intensity to obtain a similar photon flux for cells loaded with each dye (except for retinal, see RESULTS). The maximal photon flux, and therefore the maximal S/N, is limited by photodamage. The photodamage limit for each probe is difficult to quantify exactly (see DISCUSSION). However, various studies (see RESULTS for FM4-64 in brain slices and also Dombeck et al. 2004; L.S., personal communication; D.A.D., personal communication) found that, in several dyes, the approximate damage thresholds occur at a similar TPF photon flux. This value set the approximate illumination intensity for each dye for maximal S/N. Because the SHG photon flux is similar to the TPF photon flux, these considerations allow us to compare the S/N simply by measuring  $\Delta S/S$  (SHG or TPF) for each probe. The  $\Delta S/S$  was measured by applying fast (millisecond time scale) voltage steps.

*Aplysia* neurons were prepared according to Dombeck et al. (2004). Brain slices were prepared as listed above. Staining of cultured neurons was accomplished by extracellular perfusion of the dyes: JPW1114 (Di-2-ANEPEQ; 25  $\mu$ M), ANNINE-6 (as in Kuhn et al. 2004), DHPESBP (as in Dombeck et al. 2004), FM4-64 (25  $\mu$ M), Di-4-ANEPPS (as in Millard et al. 2003), and Retinal (as in Nemet et al. 2004). Intracellular staining in brain slices was accomplished as listed above: DHPESBP (100–300  $\mu$ M in intracellular solution containing cyclo- $\gamma$ -dextran, to prevent dye precipitation, prepared as in Millard et al. 2003), JPW1114 (200  $\mu$ M in intracellular solution), and ANNINE-6 (1.7 mM stock in DMSO + 20% pluronic diluted 1:20 in intracellular solution; this high concentration of DMSO and pluronic was needed to adequately stain the cells, but did not noticeably affect cell viability). Line scanning and voltage clamping of *Aplysia* neurons stained with these dyes was the same as in Dombeck et al. (2004); brain slice line scanning and voltage clamping is described above. The following excitation wavelengths, SHG and TPF emission filters, and average powers at the sample were used to measure SHG and TPF  $V_m$  sensitivities: JPW1114 [1,064 nm, 570/150 (TPF), 530/30 (SHG), 60 mW], ANNINE-6 [980 nm, 570/150 (TPF), 30 mW; 1,064 nm, 570/150 (TPF), 530/30 (SHG), 80 mW], DHPESBP [940 nm, 575/150 (TPF), 460/30 (SHG), 15 mW], FM4-64 [1,064 nm, 570/150 (TPF), 530/30 (SHG), 15 mW], Di-4-ANEPPS [850 nm, 575/150 (TPF), 425/20 (SHG), 15 mW], and retinal [900 nm, 575/150 (TPF), 460/30 (SHG), 15 mW]. The shorter wavelengths were obtained with a mode locked Ti:Sapphire laser (Spectra Physics, Tsunami). As a control, the sensitivity of ANNINE-6 was measured in HEK293 cells at 980 nm under the same conditions as Kuhn et al. (2004); our value of  $-35 \pm 2\%/100$  mV (slope at 0 mV) agrees with their value of  $-35 \pm 5\%/100$  mV. The measurement in HEK293 cells was also repeated at 1,064 nm (see DISCUSSION).

RESULTS

Staining and imaging

Neurons in hippocampal slices patch clamped and filled with intracellular solution containing FM4-64 and illuminated with  $\sim 1,064$ -nm/ $\sim 300$ -fs laser pulses generate an intense SHG signal from the labeled inner leaflet of the plasma membrane, with little background signal from intracellular or extracellular sources (compare SHG in Fig. 1A to TPF in Fig. 1B). The plasma membrane to intracellular SHG signal ratio is  $M/I = 20.3 \pm 11.8$  ( $n = 16$  cells) for soma and proximal larger dendrites. In finer dendrites and spines, the intracellular space could not be resolved, precluding measurements of this ratio. The lack of an SHG signal from intracellular membranes is likely caused by 1) dye flip-flop quickly resulting in a dye concentration equilibrium between leaflets of the intracellular membranes, destroying the asymmetry needed for SHG; 2) subresolution invaginations and foldings of the intracellular membranes (Krstić 1979; Ladinsky et al. 1999), leading to destructive SHG interference from oppositely oriented dye molecules; or 3) different partitioning coefficients for FM4-64 in the plasma membrane versus intracellular membranes (Sprong et al. 2001).

The staining time for FM4-64 varies depending on many parameters (whole cell access resistance, neuron volume and architecture, etc.), but typically an SHG signal from the soma and dendrites  $>100$   $\mu$ m distal from the soma was visible  $\sim 5$  and  $\sim 25$  min after whole cell break-in, respectively (Fig. 1C). Most cell bodies were  $\sim 50$ – $70$   $\mu$ m below the slice surface, with many of the stained dendrites  $>125$   $\mu$ m below the surface. Axons were also visible in some images (data not

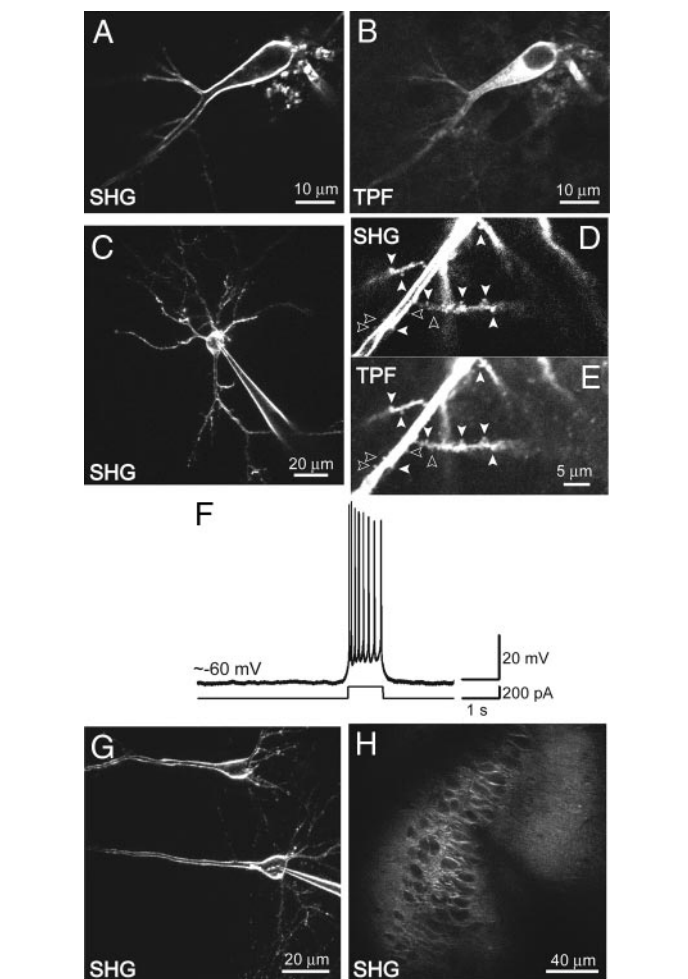


FIG. 1. Intracellular second-harmonic generation (SHG) labeling of neurons in acute rat brain slices with FM4-64. A: SHG z-section shows high membrane contrast from a neuron patch clamped and filled with FM4-64 in a hippocampal brain slice. B: 2-photon fluorescence (TPF) z-section of the same neuron as A. Note the large amount of intracellular TPF signal and poor membrane contrast. C: SHG z-projection image revealing the dendritic arbor of a neuron filled in slice with FM4-64. D: SHG z-projection image of dendrite with dendritic spines in slice from P24 rat; arrowheads pointing to spines. E: TPF z-projection of the same region shown in D. Filled arrowheads point to spines seen in both SHG and TPF; open arrowheads point to those seen only in TPF. F: current-clamp recording,  $\sim 45$  min after whole cell patch break-in, from the neuron seen in C shows physiologically normal parameters. G: 2 cells are labeled in the same field of view to show a method of population labeling. H: to show SHG labeling of many cells, this hippocampal cell layer was labeled by pressure injection of FM4-64.

shown). Current-clamp recordings from stained cells reveal physiologically normal parameters: resting potential of approximately  $-65 \pm 10$  mV, input resistance of  $\sim 150$  M $\Omega$  to 2 G $\Omega$ , AP amplitudes of  $\sim 65$ – $100$  mV, and duration of  $\sim 1.0 \pm 0.5$  ms. Figure 1F shows a current-clamp recording from a stained neuron  $\sim 45$  min after whole cell break-in. Average whole cell recordings lasted  $\sim 45$  min, with some cells viable for  $>1.5$  h, similar to cell viability without imaging or dye. Toward the end of recordings, many cells had an increased diffuse intracellular SHG signal. Additionally, a fraction ( $\sim 25\%$ ) of otherwise normal neurons had a greater intracellular SHG signal ( $M/I \sim 5$ ) throughout the recording time.

The high spatial resolution ( $\sim 0.6$   $\mu$ m) allows for dendritic spine visualization. A comparison between SHG (Fig. 1D) and

TPF (Fig. 1E) spine images reveals that not all of the spines visible in the TPF channel are visible in the SHG channel. The filled arrowheads point to spines visible in both channels, whereas the open arrowheads point to spines visible only in the TPF channel. No spines were present in only the SHG and not the TPF channel. It is possible that the size of individual spines and/or the distance between adjacent spines leads to destructive interference of the SHG signal in some cases. Multi-cell labeling is also possible. Figure 1G shows two neurons patch clamped and filled in the same field of view, whereas Fig. 1H shows a larger population stained by pressure injecting a concentrated solution of FM4-64 into the CA1 cell layer. Although *M/I* appears to be greater than stated above in many figures (Figs. 1, 3, 4), this is an illusion caused by projecting many *z*-sections onto one plane.

*Response of SHG to fast V<sub>m</sub> transients*

By applying voltage steps to the voltage-clamped neurons during line scanning, we found that the SHG signal is modulated by  $\Delta V_m$  on the physiologically relevant (~1 ms) time scale (Fig. 2, A–C). A linear response of the SHG signal with respect to  $\Delta V_m$  [linear best fit:  $\Delta\text{SHG}/\text{SHG} = (0.075\%/mV)\Delta V_m$ ; slope error = 0.004%/mV] is observed by applying a range of voltage steps (Fig. 2D). The SHG signal increases with positive voltage steps and decreases with negative voltage steps, opposite to the response seen from extracellularly labeled neurons in culture. This is expected from the opposite orientation of the chromophore with respect to the transmembrane electric field.

*Spatial resolution and S/N*

Assuming a shot noise limited system, the S/N for  $V_m$  recording can be written

$$\frac{S}{N} \propto \frac{\Delta S}{S} \sqrt{n \cdot \phi \cdot t} \tag{1}$$

where  $\Delta S/S$  is the normalized relative signal response to  $\Delta V_m$  ( $V_m$  sensitivity),  $n$  is the number of averaged line scans,  $\phi$  is the number of detected photons/time, and  $t$  is the time the focal volume scans over the membrane per line;  $t$  is defined by  $t = a/v$ , where  $a$  is the distance scanned over the membrane, and  $v$  is the focal volume scanning velocity. Line scanning perpendicular to the membrane ( $t \sim 10 \mu\text{s}$ ,  $a$  reduces to the focal volume diameter) provides high spatial resolution ( $\sim 0.6 \mu\text{m}$ ; Fig. 2, A–C) and results in S/N for a single line scan of  $\sim 1$  for a 90-mV step and S/N of  $\sim 5$  for temporal averaging of  $n = 50$  line scans. The shot noise corresponds to  $\sim 100$  photons/membrane pass ( $\sim 10$  photons/ $\mu\text{s}$  on the membrane) and  $\sim 5,000$  photons after averaging. Line scanning parallel to (along) the neuronal membranes is also used (Figs. 3 and 4); this amounts to increasing  $a$ . The differences in S/N for fast SHG  $V_m$  recordings seen in this research are caused by one or more of the following: number of line-scans averaged ( $n$ ), integration time on the membrane ( $t$ ), average illumination intensity ( $I$ ), degree of staining, polarization of the incident illumination with respect to membrane position, and/or  $\Delta V_m$  in the specific recording.

*Detection of APs and fast voltage steps*

To prove the ability of SHG to record fast neuronal  $V_m$  signals in brain slices, APs were elicited and optically recorded. The line scanning position parallel to the somatic membrane is shown in Fig. 3A. Two  $\sim 1$ -ms APs were elicited by current injection through the patch pipette during line-scanning. Line scan averaging ( $n = 55$ ) showed that optical intensity modulations in the SHG emission (Fig. 3B) occur during the AP time-course (Fig. 3C) with S/N  $\sim 7$ –8, 0.83-ms

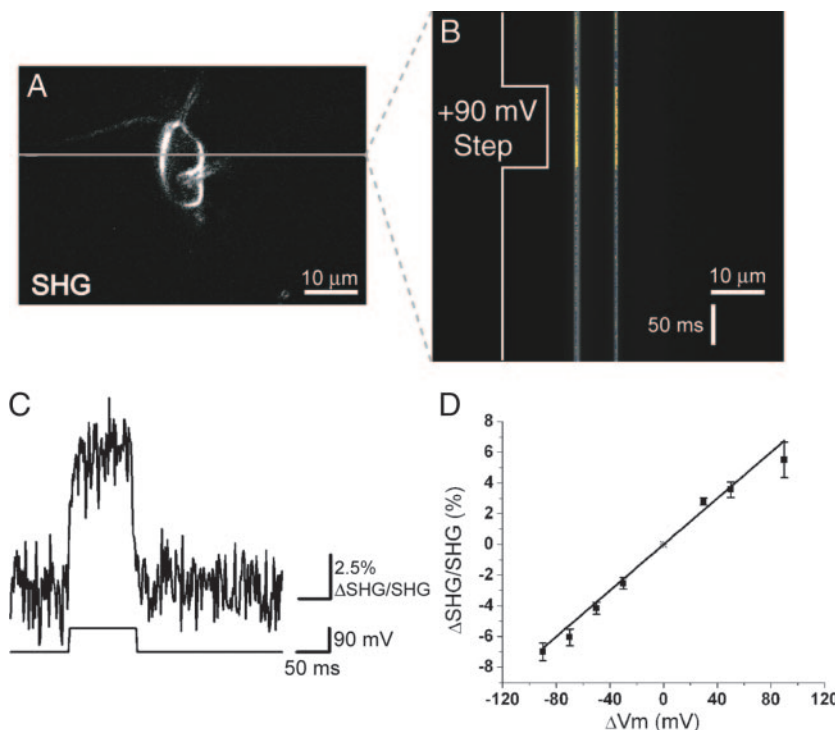


FIG. 2. SHG line scan recording of  $V_m$  during voltage steps in a patch-clamped neuron filled with FM4-64 in a brain slice. A: SHG *z*-section through the soma of a patched neuron. Patch pipette is seen protruding into this *z*-section. Gray line represents scanned line where  $V_m$  was recorded. B: SHG signal changes recorded by line scanning the line denoted in A at 600 lines/s. Voltage-clamped neuron was given a 100-ms duration, +90-mV step after 90 ms of scanning during each line scan.  $n = 50$  line scans were averaged. Line scan image is scaled to visualize the small increase in SHG emission (yellow). C: *top*: obtained from the left membrane SHG line in B, is an intensity plot of SHG emission vs. time. *Bottom*: command voltage during voltage clamp. D: plot of  $\Delta\text{SHG}/\text{SHG}$  over physiologically relevant  $\Delta V_m$ . Functional fit shows a linear relationship. Error bars represent SD of 3–7 different measurements at each  $\Delta V_m$ .

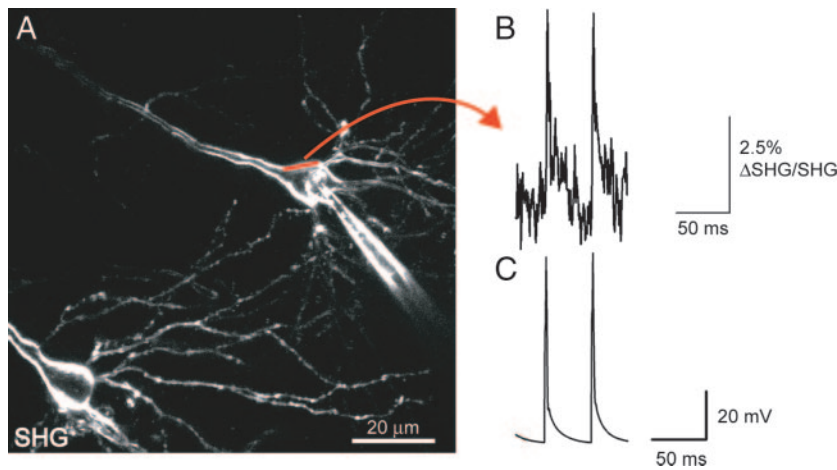


FIG. 3. Fast SHG line scan recording of elicited APs in brain slice. *A*: to show recording of action potentials (APs) with SHG, this neuron was patch clamped and filled with FM4-64. Straight red line represents scanned line where elicited APs were recorded optically by integrating over the width. *B*: SHG recording of APs with S/N of  $\sim 7$ – $8$ . This intensity plot of SHG emission vs. time is obtained from averaged line scans (1,200 lines/s) of the line denoted in *A*.  $n = 55$  line scans were averaged. *C*: average current-clamp trace of elicited APs recorded optically in *B*.

temporal, and  $0.6 \mu\text{m}$  by  $\sim 7 \mu\text{m}$   $x$ - $y$  spatial resolution. Trains up to four APs were recorded in other experiments (data not shown). The temporal resolution of the scanning system is approximately the same as the AP duration; this

can result in undersampled recordings. It is possible, however, to record the approximate AP peak voltage optically by synchronizing the time of the AP peak and the focal volume recording time on the membrane ( $t$ ). Asynchrony in

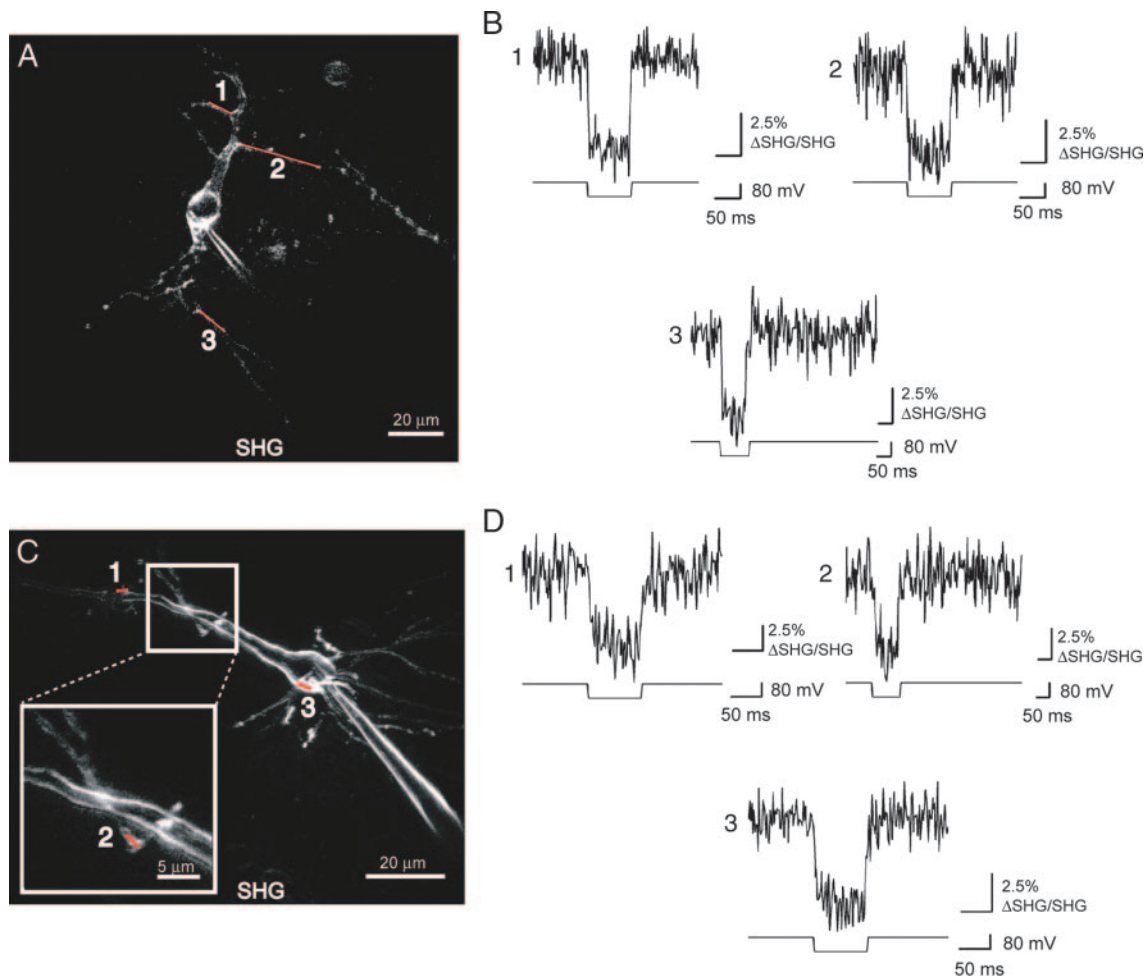


FIG. 4. Fast SHG line scan recordings from multiple sites in the dendritic arbor of neurons in brain slice. *A*: to show fast SHG recordings of  $V_m$  from the dendritic arbor, neurons were filled with FM4-64, and line scan recordings were made from positions denoted by red lines, by integrating over the width, while voltage steps were applied at the soma. *B*: *top*: intensity plot of SHG emission vs. time for lines denoted in *A*. 1)  $n = 60$  line scans were averaged with a recording speed of 600 lines/s. 2)  $n = 30$  line scans were averaged with a recording speed of 600 lines/s. 3)  $n = 30$  line scans were averaged with a recording speed of 300 lines/s. *Bottom*: command voltage applied at the soma. *C*: SHG projection image of another neuron with red lines representing the line scan positions where  $V_m$  was recorded. *D*: *top*: intensity plot of SHG emission vs. time for lines denoted in *C*. 1)  $n = 35$  line scans were averaged with a recording speed of 600 lines/s. 2)  $n = 35$  line scans were averaged with a recording speed of 300 lines/s. 3)  $n = 35$  line scans were averaged with a recording speed of 600 lines/s. *Bottom*: command voltage applied at the soma.

this regard results in SHG traces not recording the AP peak voltage.

Figure 4 shows the ability to record fast  $V_m$  events in the dendritic arbor using SHG. Scanning positions parallel to dendritic and somatic membranes on two neurons in slice are shown. During line scanning, voltage steps were applied through the patch pipette at the soma. After line scan averaging ( $n \geq 30$ ), the S/N varied between  $\sim 3.5$  and 5.0. Many of the probed dendrites were  $< 2 \mu\text{m}$  in diameter and  $\sim 100 \mu\text{m}$  below the slice surface. The recording plane for the oblique dendrite in Fig. 4C (*inset*) is actually  $\sim 30 \mu\text{m}$  above the apical dendrite seen in this  $z$ -projection image.

Photodamage was seen during some FM4-64 SHG AP recordings when a dose corresponding to  $I \sim 7 \text{ MW}/\text{cm}^2$  and  $t \sim 65 \mu\text{s}$  was reached. In many cases below this dose, the damage is negligible in comparison with nonimaging controls, as determined by AP amplitude and duration stability, resting potential stability, and absence of gross morphological changes. The dendritic arbor is more sensitive to photodamage than the soma, so the dose in the arbor was reduced compared with that used at the soma. It was also found that increasing the time between each individual line scan during averaging helped reduce photodamage. Many seconds ( $\sim 5 \text{ s}$ ) works well, but many successful recordings were also made with  $\sim 2 \text{ s}$  between scans.

*Backward-directed SHG component*

In addition to the large forward propagating SHG signal used for recordings in this research, the stained neuronal membranes also generate a small backward directed SHG signal in slice. A SHG forward versus backward ratio of  $6.6 \pm 1.1$  was deduced from SHG images of filled neurons, both in forward and epi propagation directions, with fluorescence calibration for absorption and scattering in the tissue, and collection efficiency differences of the optics and detectors in each direction. These measurements were made 50–100  $\mu\text{m}$  deep into 250- $\mu\text{m}$ -thick brain slices from P16–P17 rats. Like the forward propagating signal, the backward signal emanates predominately from the plasma membrane, with little background. The S/N for  $V_m$  recording with the SHG backward-directed component is reduced by a factor of  $\sim \sqrt{6.6}$  compared with the SHG forward propagating signal.

*Staining and  $V_m$  sensitivity with various TPF and SHG optical probes*

We initially compared the optical  $V_m$  recording S/N for many of the best known SHG and TPF  $V_m$  probes in cultured *Aplysia* neurons (stained by extracellular perfusion of the dyes) to select the best candidates for use in intact brain tissue: ANNINE-6, FM4-64, DHPESBP, Di-4-ANEPPS, JPW1114, and retinal. The most important parameter for comparing these dyes is the S/N, which depend on many parameters (see Eq. 1); however, we found that the S/N was most strongly related to  $\Delta S/S$  (see METHODS), making it possible to compare the S/N simply by measuring  $\Delta S/S$  (SHG or TPF) for each probe.

Although retinal (Nemet et al. 2004) showed a high SHG  $\Delta S/S$  ( $\sim 20\%/100 \text{ mV}$ ), the S/N was reduced by an effective SHG cross-section far lower than the other probes that could not be overcome because of poor staining efficiency and severe photobleaching problems. In contrast to the measurements

performed by Millard et al. (2003, 2004) on the slow (seconds) time scale, no SHG response to fast (milliseconds)  $\sim 100\text{-mV}$  voltage steps was seen from neurons stained with DI-4-ANEPPS, and the TPF  $\Delta S/S$  was  $\sim 3\%/100 \text{ mV}$ . This result implies that there is no correlation between fast (electro-optic or reorientational; Moreaux et al. 2003; Pons et al. 2003) and slow SHG  $V_m$  response mechanisms. The largest  $\Delta S/S$  was measured in culture with ANNINE-6, FM4-64, DHPESBP, and JPW1114. The membrane staining ability and  $\Delta S/S$  (SHG and TPF) of these four probes in culture are summarized in the first column of Fig. 5 and in Dombeck et al. (2004) and Moreaux et al. (2003).

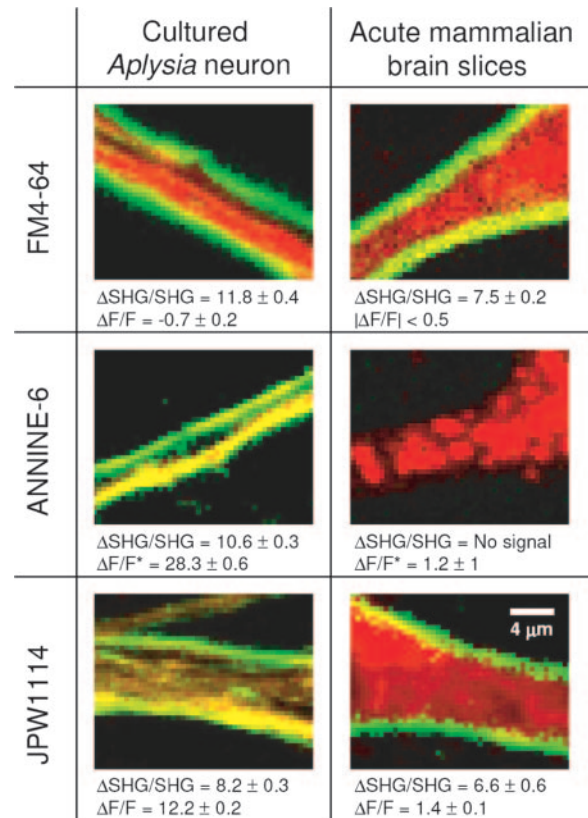


FIG. 5. Direct experimental comparison between SHG (green pseudo-color) and TPF (red pseudo-color) for  $V_m$  recording. The 3 most promising dyes for nonlinear microscopy  $V_m$  detection (FM4-64, ANNINE-6, and JPW1114) were compared at 1,064-nm excitation by their  $V_m$  sensitivity ( $\Delta S/S$ ) on the fast time scale and ability to stain the plasma membrane in cultured neurons and acute brain slices. Cultured *Aplysia* neurons, left column: in extracellularly labeled cultured *Aplysia* neurons, the TPF background can be kept low, making it possible to compare more directly the SHG and TPF  $\Delta S/S$  ( $\Delta\text{SHG}/\text{SHG}$  and  $\Delta F/F$  shown in  $\%/100 \text{ mV}$ ). SHG is generated with all of the probes, indicating a high membrane labeling efficiency. A yellow color from the short membrane stretches indicates an overlap of TPF (red) and SHG (green). It was found that FM4-64 has the highest SHG  $\Delta S/S$ , whereas ANNINE-6 has the highest TPF  $\Delta S/S$ . \*Note that ANNINE-6 TPF was measured at 980 nm to compare with the work by Kuhn et al. (2004). Acute brain slices, right column: in intracellularly filled acute brain slices, the  $\Delta S/S$  results change drastically. Here it is seen that filling neurons in slice with ANNINE-6 leads to poor membrane staining (no SHG is seen), resulting in an  $\sim 23$  times reduction in the effective  $\Delta S/S$  compared with culture. As seen by the SHG signal, high membrane labeling efficiency was possible with FM4-64 and JPW1114 in brain slices. With these signals, it is possible to measure a similar SHG  $\Delta S/S$  and signal-to-noise ratio (S/N) compared with culture. It is important to realize that even with high membrane labeling efficiency, the TPF  $\Delta S/S$  from JPW1114 is still drastically reduced by an order of magnitude compared with culture. The sign of  $\Delta S/S$  seen in extracellularly stained cultured cells and intracellularly filled neurons is the same because the opposite  $\Delta V_m$  was applied through the electrodes.

Given the  $\Delta S/S$  from our culture dish experiments, we focused our brain slice studies on the four best probes. DHPESBP was eliminated because neurons in slice filled with this dye showed no SHG from intracellular or plasma membranes, indicating poor membrane labeling compared with in culture. The membrane staining ability and  $\Delta S/S$  (TPF and SHG) of ANNINE-6, FM4-64, and JPW1114 probes in brain slice are summarized in the second column of Fig. 5. It is seen that ANNINE-6 was not able to produce SHG in brain slices, again indicating little dye partitioning into the plasma membrane. Because of the large TPF  $\Delta S/S$  seen in extracellularly stained cultured cells, we were encouraged to measure the  $\Delta S/S$  in filled neurons. This measurement showed a drastic reduction of the TPF  $\Delta S/S$  from 28.3%/100 mV in cultured neurons to 1.2%/100 mV in brain slices. A large reduction of the TPF  $\Delta S/S$  (from 12.2%/100 mV in cultured neurons to 1.4%/100 mV in brain slices) is also shown for JPW1114; however, the JPW1114 brain slice SHG signal seen in Fig. 5 shows this dye is well loaded into the membrane. This indicates that the high background and low membrane contrast, rather than poor membrane loading, is responsible for the reduced TPF  $\Delta S/S$ . On the other hand, the SHG  $\Delta S/S$  of FM4-64 and JPW1114 is only slightly affected by intracellular brain slice loading compared with the culture dish. Additionally, FM4-64 presented a higher SHG  $\Delta S/S$  and slower flip-flop rate between leaflets of the membrane than JPW1114. These results show that the best  $\Delta S/S$ , and consequently S/N, in brain slice is obtained with FM4-64 SHG.

## DISCUSSION

### *S/N and photodamage considerations*

Increases in S/N are dependent on 1) increasing  $\phi$  in Eq. 1 to decrease the shot noise and/or 2) increasing  $\Delta S/S$  in Eq. 1. Both 1 and 2 can be accomplished through the design of better dye molecules. This is the subject of current experiments in our laboratory and reports of others (Barzoukas et al. 1996; Millard et al. 2004; Moreaux et al. 2003; Nemet et al. 2004; Pons et al. 2003). It is hoped that design and screening of many SHG probes on the physiologically relevant fast time scale will soon lead to similar increases in SHG  $\Delta S/S$  and low bleaching as have been reported for TPF from ANNINE-6 (Kuhn et al. 2004). Other incremental increases in point 1 above have been made and will continue to be sought through the engineering of higher transmission optics and higher quantum yield photo-detectors (such as the GaAsP detectors used here).

With respect to FM4-64 and the current photon collection/detection technology, the factor most limiting S/N is photodamage, and in fact, the shown S/N in Figs. 2–4 was obtained near the damage thresholds for soma and dendrite recordings. Studies aimed at understanding and decreasing this problem should help to increase S/N by accommodating increases in incident laser intensity that will increase  $\phi$ . Photodamage is not well understood, and its source remains an open question (Zipfel et al. 2003b), although it is generally agreed that this damage stems from absorption of the incident illumination. Damage during SHG is likely therefore to stem from absorption and nonradiative photoproducts of the chromophore. The damage is a complicated function of  $I$ ,  $t$ , staining, cell morphology, and other unknown factors (Hopt and Neher 2001;

Koester et al. 1999), and here was found to vary from cell to cell and even within one cell. A study is underway in our laboratory to characterize the photodamage and possibly to reduce its influence through the use of antioxidants. The results of this study may also increase S/N enough for the detection of fast  $V_m$  events in a single trial.

To detect  $V_m$  signals of 100 mV optically in a single trial using SHG from FM4-64 with S/N = 5, it would be necessary to collect  $\sim 4,500$  photons per membrane recording time  $t$ . This could be accomplished given the SHG  $\phi$  and  $\Delta S/S$  shown here for FM4-64, with the only change being an increase in  $t$  to  $\sim 450 \mu\text{s}$ . In the line scanning configuration, this integration time could be achieved by increasing  $a$ , the distance scanned over the membrane; however, this was found to cause photodamage in brain slices unless  $I$  was simultaneously reduced. For this reason, damage studies, better photo-detectors, and/or higher effective cross-section dye molecules are needed to increase the number of collected photons. Improvements in dye molecule performance can also increase  $\Delta S/S$ . Assuming a dye with  $\Delta S/S \sim 20\%/100$  mV, the number of collected photons needed to measure a 100-mV  $V_m$  signal optically with S/N = 5 is  $\sim 600$  photons per membrane recording time  $t$ . If we also assume a fourfold increase in  $\Phi$  over that shown in this research for FM4-64, an integration time of  $t \sim 15 \mu\text{s}$  would be needed. Assuming the proper scanning system such as random access scanning (Bullen and Saggau 1999; Iyer et al. 2004; Otsu et al. 2005; Roorda et al. 2004), this integration time could allow for  $\sim 65$  different locations in the brain slice to be sampled at 1 kHz or  $\sim 20$  locations at 3 kHz. This shows the potential of SHG to optically record fast  $V_m$  signals at many different positions deep within scattering brain tissue.

### *Comparison of various SHG and TPF probes for $V_m$ recording*

SHG and TPF currently provide the best methods for high spatial resolution imaging deep in scattering tissue (Denk and Svoboda 1997; Denk et al. 1990; Dömbek et al. 2003; Mertz 2004; Zipfel et al. 2003a). We have compared many of the best known SHG and TPF  $V_m$  probes to select the best candidate for use in intact brain tissue. Of these probes, JPW1114 and FM4-64 can be filled into neurons in brain slice to generate an intense plasma membrane SHG signal. On the other hand, ANNINE-6 shows little dye partitioning into the membrane and high background in brain slice; consequently, we measured a TPF  $\Delta S/S$  reduction of  $\sim 23$  times compared with the culture dish experiments. It is important to observe that the TPF  $\Delta S/S$  of JPW1114 in brain slice is also drastically reduced by an order of magnitude. In this case the dye is well partitioned into the plasma membrane producing an SHG signal; however, the effective TPF  $\Delta S/S$  is still greatly affected by the poor membrane contrast and high background. Furthermore, this problem is not specific to intracellular staining; pressure injection of ANNINE-6 into brain slices also results in a low membrane contrast compared with FM4-64 SHG, likely caused by binding of the dye to extracellular components such as the extracellular matrix. The SHG  $\Delta S/S$  was reduced only slightly (20–30%) between the culture dish and intracellular filling in intact systems. A similar SHG  $V_m$  sensitivity dependence on the slow time scale has also been observed between different cell types (Sacconi et al. 2005). These marginal effects may be

explained by the vastly different environments of extracellular staining of *Aplysia* neurons (with a salt concentration approximately twofold greater than mammalian neurons) and intracellular staining of mammalian neurons in brain slice, small SHG background variations (see *M/I* measurements above), or possibly by the different physical and chemical properties of the plasma membrane environments.

These results show that 1) the SHG  $\Delta S/S$  is not degraded by background signal (as is TPF), and consequently, the S/N is greater by almost an order of magnitude with SHG than TPF using currently known probes in brain slices; 2) together with the linear response to  $\Delta V_m$ , the low SHG background makes it possible to quantify directly the SHG  $V_m$  response in terms of  $\Delta V_m$ . This is more difficult with TPF because of spatial variations in the background (see Fig. 5 or Antic and Zecevic 1995); 3) the SHG  $\Delta S/S$  is more consistent in different cell types and staining environments than TPF; and 4) of the tested nonlinear optical  $V_m$  probes, the best S/N achieved in brain slice is provided by FM4-64 SHG.

Our results suggest that it will be difficult to increase the TPF membrane contrast, given the JPW1114 results. Therefore the most promising direction to follow to increase the optical  $V_m$  recording S/N with nonlinear microscopy in intact systems is to increase  $\Delta S/S$  and/or the effective cross-section of SHG or TPF probes. Simply increasing the TPF  $\Delta S/S$  and/or cross-section of probes such as ANNINE-6 or JPW1114 without considering the TPF background will likely not lead to a solution to the problem. For example, to overcome this background problem, a TPF  $\Delta S/S \sim 20$  times greater than ANNINE-6 would be needed. According to Kuhn et al. (2004), increases in  $\Delta S/S$  for ANNINE-6 should be possible at longer wavelengths. Although our  $\Delta S/S$  measurements at 980-nm agree with Kuhn et al. (see METHODS), under the same conditions we measure only an  $\sim 30.8 \pm 1\%/100\text{-mV}$  sensitivity at 1,064 nm. Together, these arguments and results imply that the most promising direction of engineering to follow for nonlinear microscopy  $V_m$  recording is to increase the  $\Delta S/S$  and effective cross-section of SHG probes.

For in vivo applications a large fraction of the TPF signal can be epi-collected, whereas only a small fraction of the SHG signal can be collected in this direction. Wavelength scale inhomogeneities (Mertz and Moreaux 2001) or secondary scattering of the forward propagating SHG signal are the likely cause of the backward propagating SHG signal. The longer scattering length presented to the forward propagating SHG photons in vivo compared with in slice may increase the SHG backward scattered signal. New technologies to manipulate the polarization and phase of the illumination light within the focal volume (Novotny et al. 2001) may also increase the SHG backward propagating signal by optimizing coherent addition conditions. Even if the backward propagating SHG signal cannot be increased in the future, currently the S/N for intact systems  $V_m$  recording with back propagating FM4-64 SHG is still approximately three times better than can be achieved with ANNINE-6 epi-collected TPF and approximately the same as JPW1114 epi-collected TPF. In theory, combining the epi-TPF and back-propagating SHG signals from JPW1114 may provide a slight advantage over FM4-64 in vivo; however, the rapid flip-flop rate of JPW1114 compared with FM4-64 must also be considered.

### Possible applications and future directions

Micron scale  $V_m$  dynamics deep in intact neural systems, where much of the volume of activity and dendritic integration resides, have been inaccessible until now because of the light scattering limitations of linear optical methods. We have shown the optical recording of fast neuronal  $V_m$  transients deep in intact mammalian neural tissue with micron scale resolution using SHG microscopy from targeted neurons patch clamped and filled with FM4-64. This technique should find applications in the near future in studies that directly record and quantify fast  $\Delta V_m$  from dendritic spines (Tsay and Yuste 2004) and from fine dendrites. Deeper single cell patching/SHG recording can be implemented using TPF targeted patch clamping (Margrie et al. 2003). Because the SHG emission is always at one-half the illumination wavelength, it can also be combined easily with functional fluorescent indicators such as  $\text{Ca}^{2+}$ - and  $\text{Na}^{+}$ -sensitive dyes. With further improvements in the S/N, labeling methods (Hinner et al. 2004), and a combination with faster and more flexible imaging modalities (Bullen and Saggau 1999; Iyer et al. 2004; Kobayashi et al. 2002; Otsu et al. 2005; Roorda et al. 2004; Sacconi et al. 2003; Tsien and Bacskaï 1995), SHG should move the imaging field closer to large scale high-resolution  $V_m$  recordings of population activity deep in thick tissue preparations.

### ACKNOWLEDGMENTS

We thank T. Mallegol for the synthesis of the DHPESBP dye, S. Kim, R. Molloy, M. Williams, and R. Williams for helpful discussions and reading of this manuscript, W. Zipfel and I. Tullis for instrumentation support, and R. Yuste for helpful discussions on the intracellular use of FM4-64. We also thank R. Harris-Warrick, M. Diaz-Rios, and D. Tsay for slice patch clamping advice and guidance and H. Vishwasrao and K. Kasischke for advice on slice preparation.

### GRANTS

M. Blanchard-Desce is grateful to CNRS for financial support (Action Coordonnée Optique and Physique et Chimie du Vivant grants), L. Sacconi is grateful to the European Laboratory for Non-Linear Spectroscopy for Grant MTKD-CT-2004-509761 and to Cornell University for his visit, and D. A. Dombeck and W. W. Webb are grateful for funding from National Institutes of Health Grants P41 EB-001976-17, GM-08267, and GM-07469.

### REFERENCES

- Antic S and Zecevic D. Optical signals from neurons with internally applied voltage-sensitive dyes. *J Neurosci* 15: 1392–1405, 1995.
- Antic SD. Action potentials in basal and oblique dendrites of rat neocortical pyramidal neurons. *J Physiol* 550: 35–50, 2003.
- Barzoukas M, Runser C, Fort A, and Blanchard-Desce M. A two-state description of (hyper)polarizabilities of push-pull molecules based on a two-form model. *Chem Phys Lett* 257: 531–537, 1996.
- Bouevitch O, Lewis A, Pinevsky I, Wuskell JP, and Loew LM. Probing membrane potential with nonlinear optics. *Biophys J* 65: 672–679, 1993.
- Bullen A and Saggau P. High-speed, random-access fluorescence microscopy. II. Fast quantitative measurements with voltage-sensitive dyes. *Biophys J* 76: 2272–2287, 1999.
- Campagnola PJ, Wei MD, Lewis A, and Loew LM. High-resolution nonlinear optical imaging of live cells by second harmonic generation. *Biophys J* 77: 3341–3349, 1999.
- Cohen LB, Keynes RD, and Hille B. Light scattering and birefringence changes during nerve activity. *Nature* 218: 438–441, 1968.
- Denk W, Strickler JH, and Webb WW. Two-photon laser scanning fluorescence microscopy. *Science* 248: 73–76, 1990.
- Denk W and Svoboda K. Photon upmanship: why multiphoton imaging is more than a gimmick. *Neuron* 18: 351–357, 1997.
- Djurisic M, Antic S, Chen WR, and Zecevic D. Voltage imaging from dendrites of mitral cells: EPSP attenuation and spike trigger zones. *J Neurosci* 24: 6703–6714, 2004.

- Dombeck DA, Blanchard-Desce M, and Webb WW.** Optical recording of action potentials with second-harmonic generation microscopy. *J Neurosci* 24: 999–1003, 2004.
- Dombeck DA, Blanchard-Desce M, and Webb WW.** Fast optical recording of neuronal membrane potential transients in acute mammalian brain slices by second harmonic generation microscopy. In: *Imaging Neurons and Neural Activity: New Methods, New Results*. Meeting, March 10–13, Cold Spring Harbor, NY, 2005a.
- Dombeck DA, Blanchard-Desce M, and Webb WW.** Fast optical recording of neuronal membrane potential transients in acute mammalian brain slices by second-harmonic generation microscopy. Biophysical Society Annual Meeting, February 12–16, Long Beach, CA, 2005b, p. 363a.
- Dombeck DA, Kasischke KA, Vishwasrao HD, Ingelsson M, Hyman BT, and Webb WW.** Uniform polarity microtubule assemblies imaged in native brain tissue by second-harmonic generation microscopy. *Proc Natl Acad Sci USA* 100: 7081–7086, 2003.
- Gonzalez JE and Tsien RY.** Improved indicators of cell membrane potential that use fluorescence resonance energy transfer. *Chem Biol* 4: 269–277, 1997.
- Grinvald A and Hildesheim R.** VSDI: a new era in functional imaging of cortical dynamics. *Nat Rev Neurosci* 5: 874–885, 2004.
- Hinner M, Huebener G, and Fromherz P.** Genetic targeting of fluorescent voltage-sensitive dye by enzymatically induced membrane binding. Society for Neuroscience Annual Meeting, November 12–18, San Diego, CA, 2004.
- Hopt A and Neher E.** Highly nonlinear photodamage in two-photon fluorescence microscopy. *Biophys J* 80: 2029–2036, 2001.
- Iyer V, Hoogland T, Losavio B, Fink R, Gaddi R, Patel S, Larson A, and Saggau P.** Acousto-optic multiphoton laser scanning microscopy (AO-MPLSM) in living brain slices: structural and functional imaging. *Society for Neuroscience Annual Meeting*, November 12–18, San Diego, CA, 2004, p. Program No. 849.819.
- Kay AR, Alfonso A, Alford S, Cline HT, Holgado AM, Sakmann B, Snitsarev VA, Stricker TP, Takahashi M, and Wu LG.** Imaging synaptic activity in intact brain and slices with FM1-43 in *C. elegans*, lamprey, and rat. *Neuron* 24: 809–817, 1999.
- Kirov SA, Petrak LJ, Fiala JC, and Harris KM.** Dendritic spines disappear with chilling but proliferate excessively upon rewarming of mature hippocampus. *Neuroscience* 127: 69–80, 2004.
- Knopfel T, Tomita K, Shimazaki R, and Sakai R.** Optical recordings of membrane potential using genetically targeted voltage-sensitive fluorescent proteins. *Methods* 30: 42–48, 2003.
- Kobayashi M, Fujita K, Kaneko T, Takamatsu T, Nakamura O, and Kawata S.** Second-harmonic-generation microscope with a microlens array scanner. *Opt Lett* 27: 1324–1326, 2002.
- Koester HJ, Baur D, Uhl R, and Hell SW.** Ca<sup>2+</sup> fluorescence imaging with pico- and femtosecond two-photon excitation: signal and photodamage. *Biophys J* 77: 2226–2236, 1999.
- Krstić RV.** *Ultrastructure of the Mammalian Cell: An Atlas*. Berlin, NY: Springer-Verlag, 1979.
- Kuhn B, Fromherz P, and Denk W.** High sensitivity of Stark-shift voltage-sensing dyes by one- or two-photon excitation near the red spectral edge. *Biophys J* 87: 631–639, 2004.
- Ladinsky MS, Mastronarde DN, McIntosh JR, Howell KE, and Staehelin LA.** Golgi structure in three dimensions: functional insights from the normal rat kidney cell. *J Cell Biol* 144: 1135–1149, 1999.
- Margrie TW, Meyer AH, Caputi A, Monyer H, Hasan MT, Schaefer AT, Denk W, and Brecht M.** Targeted whole-cell recordings in the mammalian brain in vivo. *Neuron* 39: 911–918, 2003.
- Mertz J.** Nonlinear microscopy: new techniques and applications. *Curr Opin Neurobiol* 14: 610–616, 2004.
- Mertz J and Moreaux L.** Second-harmonic generation by focused excitation of inhomogeneously distributed scatterers. *Opt Commun* 196: 325–330, 2001.
- Millard A, Jin L, Lewis A, and Loew L.** Direct measurement of the voltage sensitivity of second-harmonic generation from a membrane dye in patch-clamped cells. *Opt Lett* 28: 1221–1223, 2003.
- Millard AC, Jin L, Wei MD, Wuskell JP, Lewis A, and Loew LM.** Sensitivity of second harmonic generation from styryl dyes to transmembrane potential. *Biophys J* 86: 1169–1176, 2004.
- Milojkovic BA, Radojicic MS, Goldman-Rakic PS, and Antic SD.** Burst generation in rat pyramidal neurones by regenerative potentials elicited in a restricted part of the basilar dendritic tree. *J Physiol* 558: 193–211, 2004.
- Moreaux L, Pons T, Dambrin V, Blanchard-Desce M, and Mertz J.** Electro-optic response of second-harmonic generation membrane potential sensors. *Opt Lett* 28: 625–627, 2003.
- Nemet BA, Nikolenko V, and Yuste R.** Second harmonic imaging of membrane potential of neurons with retinal. *J Biomed Optics* 9: 873–881, 2004.
- Novotny L, Beversluis MR, Youngworth KS, and Brown TG.** Longitudinal field modes probed by single molecules. *Phys Rev Lett* 86: 5251–5254, 2001.
- Otsu Y, Bormuth V, Ng J, and Dieudonne S.** Ultrafast multisite recording with a random access TPLSM. In: *Imaging Neurons and Neural Activity: New Methods, New Results*. Meeting, March 10–13, Cold Spring Harbor, NY, 2005.
- Pons T, Moreaux L, Mongin O, Blanchard-Desce M, and Mertz J.** Mechanisms of membrane potential sensing with second-harmonic generation microscopy. *J Biomed Optics* 8: 428–431, 2003.
- Roorda RD, Hohl TM, Toledo-Crow R, and Miesenbock G.** Video-rate nonlinear microscopy of neuronal membrane dynamics with genetically encoded probes. *J Neurophysiol* 92: 609–621, 2004.
- Sacconi L, D'Amico M, Vanzi F, Biagiotti T, Antolini R, Olivetto M, and Pavone FS.** Second-harmonic generation sensitivity to transmembrane potential in normal and tumor cells. *J Biomed Optics* 10: 24014–24018, 2005.
- Sacconi L, Froner E, Antolini R, Taghizadeh MR, Choudhury A, and Pavone FS.** Multiphoton multifocal microscopy exploiting a diffractive optical element. *Opt Lett* 28: 1918–1920, 2003.
- Siegel MS and Isacoff EY.** A genetically encoded optical probe of membrane voltage. *Neuron* 19: 735–741, 1997.
- Sprong H, van der Sluijs P, and van Meer G.** How proteins move lipids and lipids move proteins. *Nat Rev Mol Cell Biol* 2: 504–513, 2001.
- Stepnoski RA, LaPorta A, Raccuia-Behling F, Blonder GE, Slusher RE, and Kleinfeld D.** Noninvasive detection of changes in membrane potential in cultured neurons by light scattering. *Proc Natl Acad Sci USA* 88: 9382–9386, 1991.
- Stosiek C, Garaschuk O, Holthoff K, and Konnerth A.** In vivo two-photon calcium imaging of neuronal networks. *Proc Natl Acad Sci USA* 100: 7319–7324, 2003.
- Stuart GJ and Sakmann B.** Active propagation of somatic action potentials into neocortical pyramidal cell dendrites. *Nature* 367: 69–72, 1994.
- Tsay D and Yuste R.** On the electrical function of dendritic spines. *Trends Neurosci* 27: 77–83, 2004.
- Tsien RY and Baekskai BJ.** Video-rate confocal microscopy. In: *Handbook of Biological Confocal Microscopy* (2nd ed.), edited by Pawley JB. New York: Plenum Press, 1995, p. 459–477.
- Yuste R, Nemet B, Jiang J, Nuriya M, and Eisenthal K.** Second harmonic generation imaging of membrane potential. *Imaging Neurons and Neural Activity: New Methods, New Results*. Meeting, March 10–13, Cold Spring Harbor, NY, 2005.
- Zipfel WR, Williams RM, Christie R, Nikitin AY, Hyman BT, and Webb WW.** Live tissue intrinsic emission microscopy using multiphoton-excited native fluorescence and second harmonic generation. *Proc Natl Acad Sci USA* 100: 7075–7080, 2003a.
- Zipfel WR, Williams RM, and Webb WW.** Nonlinear magic: multiphoton microscopy in the biosciences. *Nat Biotechnol* 21: 1369–1377, 2003b.
- Zochowski M, Wachowiak M, Falk CX, Cohen LB, Lam YW, Antic S, and Zecevic D.** Imaging membrane potential with voltage-sensitive dyes. *Biol Bull* 198: 1–21, 2000.